



Thermal shock damage resistance of a magnesia-chrome refractory
by Charles Russell Roberts

A thesis submitted in partial fulfillment of the requirements for the degree of MASTER OF SCIENCE
in Mechanical Engineering
Montana State University
© Copyright by Charles Russell Roberts (1978)

Abstract:

A bench scale experiment was developed to quantitatively determine the thermal shock damage resistance of a commercial magnesia-chrome refractory. Samples of the refractory were exposed to environmental conditions that simulated the high temperatures and thermal cycling of a magnetohydrodynamic air preheater and produced comparable maximum surface tensile stresses. Degradation of the strength and structural integrity of the refractory were assessed through measurements of changes in room temperature compressive strength, apparent porosity/bulk volume, and thermal diffusivity. The damage resistance of the refractory was found to decrease with increasing temperature levels.

STATEMENT OF PERMISSION TO COPY

In presenting this thesis in partial fulfillment of the requirements for an advanced degree at Montana State University, I agree that the Library shall make it freely available for inspection. I further agree that permission for extensive copying of this thesis for scholarly purposes may be granted by my major professor, or, in his absence, by the Director of Libraries. It is understood that any copying or publication of this thesis for financial gain shall not be allowed without my written permission.

Signature Charles R. Roberts

Date 10/2/78

THERMAL SHOCK DAMAGE RESISTANCE OF
A MAGNESIA-CHROME REFRACTORY

by

CHARLES RUSSELL ROBERTS

A thesis submitted in partial fulfillment
of the requirements for the degree

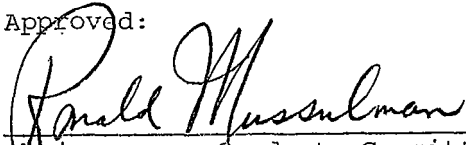
of

MASTER OF SCIENCE

in

Mechanical Engineering

Approved:


Chairperson, Graduate Committee


Head, Major Department


Graduate Dean

MONTANA STATE UNIVERSITY
Bozeman, Montana

October, 1978

ACKNOWLEDGMENTS

The author would like to thank Dr. A. J. Kumnick and Dr. R. L. Mussulman for their help and guidance in preparing this thesis. The author would also like to thank his wife Rosanne for her encouragement and understanding.

TABLE OF CONTENTS

	<u>Page</u>
VITA	ii
ACKNOWLEDGMENTS	iii
TABLE OF CONTENTS	iv
LIST OF TABLES	vi
LIST OF FIGURES	vii
ABSTRACT	viii
 Chapter	
I. INTRODUCTION	1
II. LITERATURE REVIEW	3
III. THEORY	4
Origins of Thermal Stresses	4
Microstresses	4
Macrostresses	6
Heat transfer solution	8
Thermoelastic solution	10
Thermoviscoelastic Effects	11
Brittle Fracture	12
Structural Degradation	15
IV. EXPERIMENTAL	17
Preheater Conditions	17
Specimens (RFG)	18
Development	18
Stress Model	19
Damage Assessment	22

	<u>Page</u>
Procedure	23
Apparatus	23
V. RESULTS	26
Compressive Strength	26
Visual Inspection	29
Macroscopic	29
Microscopic	30
Porosity/Bulk Volume	30
Thermal Diffusivity	31
Damage Mechanisms	34
Thermoelastic Stresses	34
Microstresses	36
Temperature	38
VI. CONCLUSIONS	39
APPENDIX	40
1. MATERIAL DESCRIPTION	41
2. DAMAGE ASSESSMENT TESTS	47
3. TEST SPECIMEN GEOMETRY	52
LITERATURE CITED	55

LIST OF TABLES

<u>Table</u>	<u>Page</u>
1. Experimental Parameters	20
2. Nominal Maximum Surface Stresses	21
3. Refractory Nominal Composition by Weight Percentage (%)	41
4. Typical Refractory Physical and Mechanical Properties	44

LIST OF FIGURES

<u>Figure</u>	<u>Page</u>
1. Experimental Apparatus	24
2. Sample Holder	25
3. Compressive Strength	27
4. Apparent Porosity	32
5. Bulk Volume	33
6. Thermal Diffusivity	35
7. Fracture Strength	45
8. Fracture Surface Energy	45
9. Resistance to Fracture	46
10. Resistance to Fracture Damage	46
11. Compressive Mounting Assembly	49
12. Test Specimens	54

ABSTRACT

A bench scale experiment was developed to quantitatively determine the thermal shock damage resistance of a commercial magnesia-chrome refractory. Samples of the refractory were exposed to environmental conditions that simulated the high temperatures and thermal cycling of a magnetohydrodynamic air preheater and produced comparable maximum surface tensile stresses. Degradation of the strength and structural integrity of the refractory were assessed through measurements of changes in room temperature compressive strength, apparent porosity/bulk volume, and thermal diffusivity. The damage resistance of the refractory was found to decrease with increasing temperature levels.

Chapter I

INTRODUCTION

Successful operation of proposed coal-fired, open cycle magneto-hydrodynamic (MHD) systems depends on the combustion air being preheated to high temperatures. This is necessary to obtain the required combustion temperatures and maximize system efficiency.

The emphasis of current MHD air preheater research has been on the development of regenerative, fixed-bed type, heat exchangers for use in directly fired systems. Particular attention has been devoted to regenerative preheaters that use cored ceramic bricks as a heat storage medium.

The operating environment of such preheaters will be severe and poses serious material problems [1]. One of these problems is the limited ability of brittle ceramics to withstand the detrimental effects of high temperatures and thermal stresses. Thermal cycling of the preheaters during operation and during startup and shutdown will introduce large, rapidly varying temperature gradients in the ceramic. Fracturing of the ceramic materials caused by the associated thermal stresses will impose constraints on both preheater design and operating life due to the degradation of ceramic structural integrity.

The refractory ceramics to be used for MHD preheater applications must possess sufficient mechanical strength stability and fracture

toughness to allow extended, high temperature, cyclic operation. That is, the material must exhibit a good resistance to thermal shock damage.

This study was undertaken to obtain a quantitative description of the damage resistance of a particular refractory under the conditions of cyclic thermal shocks and high temperatures. The material is a commercially available, rebonded fused grain magnesia-chrome refractory¹ and is presently being used as the bed material of several experimental MHD air preheaters.

A bench scale experiment was developed that was capable of producing multiple thermal shock cycles with stress levels comparable to those anticipated for an experimental preheater.² The experiment was then conducted at temperatures that span the operating temperature range of that experimental preheater, to assess the long-term degradation of the mechanical strength of the magnesia-chrome refractory.

¹Corhart RFG (RFG). For material description see Appendix 1.

²The experimental MHD air preheater at Montana State University (MSU).

Chapter II

LITERATURE REVIEW

Interest in the thermal shock damage resistances of commercial magnesia and magnesia-chrome refractories has resulted in several investigations.

Ainsworth and Herron [2] tested a number of magnesia and magnesia-chrome refractories. Specimens were subjected to 15 cycles between room temperature and 1200°C. Hicks [3] conducted a study simulating an MHD air preheater. Specimens of various high magnesia refractories were cycled between 1100-1400°C for at least 200 cycles and up to 600 cycles. Kumnick and Beezhold [4] investigated the behavior of RFG ceramic with and without high temperature impregnation of coal slag. Specimens were subjected to a single cycle between room temperature and 1450°C at varying rates of heating and cooling.

Both of the multiple thermal shock cycle investigations reported severe strength degradation within the first few cycles. After the initial strength decrease, the strength continued to degrade at a small constant rate with increasing cycles.

The study of RFG reported large changes in strength with one cycle. The more rapid cooling rates and coal slag impregnation produced the greatest changes in strength.

Chapter III

THEORY

To aid in the selection of refractory ceramics for service in an MHD air preheater, it is desirable to understand and be able to characterize the structural degradation mechanisms of high temperature thermal cycling. A major design limitation of ceramic materials is that because of their brittle nature they are susceptible to failure caused by extensive thermal stress cracking.

Origins of Thermal Stresses

Thermal stresses generated in a material are the result of differential strains produced by the nonuniform or restrained dimensional changes that accompany changing temperatures. In a polyphase ceramic body thermal stresses may be caused by several mechanisms: polymorphic phase transformations, differential thermal expansions between phases, anisotropic crystal thermal expansion in a phase, and dimensional changes due strictly to differential temperature variations in the body [5].

Microstresses

The polymorphic transformation of an unstable component phase will produce microstructural disruptions and stresses if the transformation involves a volumetric change. The magnitude of the stresses

and the extent of damage are controlled by the amount and location of the transforming phase as well as by the condition and composition of the surrounding microstructure.

The various phases present in a polyphase ceramic often exhibit markedly different coefficients of linear thermal expansion. With changing temperature the differing rates of expansion between adjacent phases result in stresses that are sufficient to cause fracturing. The following relation can be used to obtain a crude estimate of the magnitude of the stresses by considering a phase to be constrained to expand with the bulk material in all three dimensions

$$\sigma = \frac{E_i (\alpha_t - \alpha_i) \Delta T}{(1 - 2\nu)} \quad (1)$$

where: σ = triaxial stress

E_i = component phase elastic modulus

α_i = component phase coefficient of thermal expansion

α_t = bulk material coefficient of thermal expansion

ΔT = temperature change

ν = Poisson's ratio.

Crystals of a single phase can have thermal expansion coefficients along different axes that vary significantly. The random orientation of the crystals within a phase results in stress as adjacent crystals attempt to expand in any specific direction at different

rates. These stresses could also be of sufficient magnitude to fracture the microstructure.

The stresses developed by phase transformation and the differences between thermal expansion coefficients of various phases and crystallographic directions of a single phase could properly be termed microstresses. That is, they occur over extremely localized volumes within a material. The microcracking that results is also extremely localized, occurring most commonly along the grain boundaries separating phases and crystals within phases. Once formed, these microcracks serve to relieve microstresses generated in the surrounding matrix [6].

Macrostresses

The thermal stresses that are potentially the most destructive to a ceramic material are those developed by differential temperature changes. They are continuous throughout a body and, if of sufficient magnitude, can cause macroscopic cracking to the point of material failure.

This type of thermal stress is produced when the thermal expansion of the bulk material is restrained externally or when a temperature gradient causes nonuniform internal thermal expansions in the material. Stresses arising from external restraint can be avoided by providing sufficient space for thermal expansion and do not present a

serious design problem. The severity of thermal stresses caused by nonuniform internal expansions depends on the magnitude of the temperature gradient created in the material. The ability of a material to withstand these stresses limits the allowable magnitude of the temperature gradient and presents a serious design problem. The most severe stresses are produced by environmental conditions which result in large, rapidly varying temperature gradients (thermal shock).

The severity of the thermal stresses produced during thermal shock may be estimated by solving an appropriate thermoelastic stress problem. A formal theory of thermoelasticity couples the effects of heat transfer and strain rate, requiring that temperatures and deformations in a body be determined simultaneously. Formal treatments also consider the effect of inertia on the distribution of stress in a body. To obtain an expedient solution for a practical thermal stress problem, both the coupling and inertia effects are usually ignored. For most engineering applications, neglecting these effects will not introduce significant error [7,8].

Neglecting coupling and inertia effects allows a thermal stress problem to be treated as a separate heat transfer problem and a problem in quasi static thermoelasticity. Solution of the heat transfer problem will give a temperature distribution throughout a body. The temperature distribution can then be substituted into an appropriate

thermoelastic solution to obtain the distribution of stresses in a body.

Heat transfer solution. The particular geometry of the test specimen demands the use of a radial coordinate system (see experiment description). The length to diameter ratios of the specimens are sufficiently large to warrant the simplifying assumption that the cylinders are infinitely long (refer to Appendix 3 for end effect corrections).

The heat transfer boundary value problem for an infinite cylinder with a radial temperature distribution only can be formulated as follows [9]

$$\frac{1}{\alpha} \frac{\partial T}{\partial t} = \frac{1}{r} \frac{\partial}{\partial r} \left(r \frac{\partial T}{\partial r} \right) \quad (2)$$

$$T(r, 0) = T_0$$

$$-K \frac{\partial T}{\partial r} \Big|_{r=R} = hT(T(R, t) - T_{\infty})$$

$$-K \frac{\partial T}{\partial r} \Big|_{r=0} = 0$$

where: $T = T(r, t)$ temperature as a function of radial position, r , and time, t

α = thermal diffusivity

hT = total heat transfer coefficient

R = cylinder radius

T_0 = initial temperature

T_{∞} = ambient temperature.

This formulation neglects the temperature dependence of the material thermal diffusivity and thermal conductivity. Provided that these properties are weakly dependent on temperature and that the temperature differences within the cylinder are not large, this assumption does not introduce significant error.

The total heat transfer coefficient, hT , accounts for the effects of both radiation and convection heat transfer at the boundary. Radiation heat transfer is dependent on the absolute boundary temperature, $T(R, t)$, to the fourth power. This condition does not allow a conventional analytic solution to the transient boundary value problem. Instead, a solution must be obtained through some numerical method. The problem is most simply approached through a finite difference technique by dividing the cross section of the cylinder into a system of concentric, isothermal nodes. The finite difference equations required for this solution are of the form

$$T_j^{n+1} = \frac{\alpha \Delta t}{\Delta r^2} \left[AT_{j+1}^n + BT_j^n + CT_{j-1}^n \right] \quad (3)$$

and

$$T_j^{n+1} = \frac{\alpha \Delta t}{\Delta r^2} \left[\Delta T_{j-1}^n + (E + Fh \frac{\Delta r}{K}) T_j^n + Gh \frac{\Delta r}{K} T_\infty \right] \quad (4)$$

where:

$T_j^n, T_{j+1}^n, T_{j-1}^n$ = temperatures at nodes $j, j+1, j-1$ at time n

T_j^{n+1} = temperature at node j at subsequent time

A-G = numerical constants that depend on the particular nodal system and radial location at a specific node

$\Delta t, \Delta r$ = time and radial step sizes.

The second equation applies to only the surface node. Solution of this problem becomes an iterative process starting at the initial condition. For a discussion of the stability of this type of solution refer to Arpaci [9], pages 505-515.

Thermoelastic solution. The validity of formulation of a thermoelastic stress problem depends on two conditions. The deformations must be small and the material must behave elastically at the temperatures involved.

The solution to the problem of a cylindrical body with a radial temperature distribution is outlined in the literature [7]. For the case of an unrestrained infinitely long cylinder, the stress and displacement fields are

$$\sigma_{rr} = \frac{aE}{(1-\nu)} \left[\frac{1}{R^2} \int_0^R T r dr - \int_0^r T r dr \right] \quad (5)$$

$$\sigma_{\theta\theta} = \frac{aE}{(1-\nu)} \left[\frac{1}{R^2} \int_0^R T r dr + \int_0^r T r dr + T r^2 \right] \quad (6)$$

$$\sigma_{zz} = \sigma_{rr} + \sigma_{\theta\theta} \quad (7)$$

$$\sigma_{r\theta} = \sigma_{z\theta} = \sigma_{rz} = 0 \quad (8)$$

$$u(r) = \frac{a}{r(1-\nu)} \left[(1+\nu) \int_0^r T r dr + \frac{(1-3\nu)r^2}{R^2} \int_0^R T r dr \right] \quad (9)$$

$$w(z) = \frac{2az}{R^2} \int_0^R T r dr \quad (10)$$

where: σ = component stress

$u(r), w(z)$ = displacements in the radial direction r , and axial direction, z

E = modulus of elasticity

ν = Poisson's Ratio

a = coefficient of thermal expansion

T = differential radial temperature profile, $T(r,t) - T_1$

T_1 = reference temperature.

The transient temperature distributions as determined by the solution to the heat transfer problem are substituted into thermo-elastic stress equations to obtain the corresponding transient stress distributions.

Thermoviscoelastic Effects

The effect of the thermoviscoelastic behavior of a material, creep, on the thermal stresses generated under conditions of thermal shock can be neglected. The very short times required to develop maximum thermal stress levels do not allow significant stress relaxation to occur [7,10].

Brittle Fracture

Ceramic materials as a class have rigid microstructures with high moduli of elasticity. The rigidity of the microstructures will allow very little plastic deformation. Cracks forming at points of stress concentration can not easily be blunted by yielding of the surrounding material and will tend to propagate. Material failure due to this type of behavior is classified as "brittle fracture."

The majority of theoretical and experimental work in this area has been directed towards describing the thermal shock behavior of ceramic materials in terms of their physical properties and environmental conditions. Various relations have been proposed to characterize the resistance of ceramic materials for the two distinct stages of fracture, crack initiation and crack propagation. These fall generally into two categories, thermal stress fracture resistance parameters and thermal stress damage resistance parameters.¹

Fracture resistance parameters relate the ability of a ceramic material to withstand a specific level of thermal stress without fracturing. These parameters suggest that for a material to have a good resistance to fracture requires high values of tensile strength and thermal diffusivity combined with low values of elastic modulus and

¹Hasselmann [11] has compiled a fairly complete listing and interpretation of these parameters.

coefficient of thermal expansion. A low value of emissivity is also desirable in high temperature environments.

Damage resistance parameters relate the extent of crack propagation that will occur in a material after fracture has been initiated. These parameters suggest that the degree of damage can be minimized, when crack initiation can not be avoided, by selecting a material with high values of fracture surface energy and elastic modulus and a low value of tensile strength.

The damage resistance parameters assume that the energy required to create new fracture surfaces is derived from the elastic strain energy present in a body at the instant of fracture. The effective fracture surface energy is a measure of the cohesive binding forces and energy absorption mechanisms of a material's microstructure. Materials with high surface energies will sustain severe thermal shocks with less damage.

The parameters describing the fracture damage resistance of ceramic materials are strictly applicable only to thermal stress states just severe enough to initiate fracture. For cases where the thermal stresses exceed the fracture stress, kinetic and quasi static crack propagation must be considered. Hasselman [12] has developed a theory capable of accounting for those modes of crack propagation and more accurately estimating the degree of damage.

Other approaches to thermal stress fracture have been based on Weibull's statistical theory of strength [12]. Statistical concepts have been used to account for the volumetric effect on fracture and material property variability to predict the reliability of a material under conditions of thermal shock.

All of the theoretical approaches mentioned thus far have been intended to estimate the damage to, or the reliability of a material subjected to a single thermal shock only. They have been developed for well characterized materials with simple stress distributions. For most engineering ceramics, accurate data on material properties and size and number of pre-existing flaws is either not available or available only as average values with large standard deviations. The principal usage of the brittle fracture concepts with these materials has been limited to either providing a qualitative comparison between various ceramics for a specific application or to qualitatively characterize the behavior of a particular ceramic over varying levels of single thermal shock severity [2,14,15].

At present, no theoretical models exist that will describe the effects of multiple shock cycles on a material. The long-term behavior and strength degradation of ceramic must ultimately be determined through an empirical method. The theoretical concepts may then be used to aid in the interpretation of the results.

Structural Degradation

The formation of microcracks and macrocracks on cooling after the firing of a ceramic and during subsequent thermal cycling produces thermal growth of the material. When the grains and crystals surrounding these cracks are free to expand differentially, they tend to push each other apart on heating. During cooling the expansions will not be totally reversible due to changes in the temperature and stress distributions. The result is a gradual increase of void space and bulk volume. This effect produces a slight hysteresis in the overall thermal expansion and in the thermal transport properties as the cracks open and close. This type of degradation has been referred to as thermal ratcheting [5,16].

The cracking of the microstructure and the increase of void space associated with thermal ratcheting lead to a decrease in strength of the bonding matrix of a material. The degradation of the bonding may eventually cause complete disintegration of the material or reach a point of equilibrium by allowing sufficient deformation to relieve the thermal stresses without further crack propagation.

If the severity of the thermal stresses are large, macrocracks can be formed that cause the material to fail or spall suddenly. That is, the cracking may be extensive enough to fragment the ceramic body. As the process of thermal ratcheting progresses, sudden catastrophic failure becomes less likely. Increased numbers of microcracks and

void space cause propagating macrocracks to be arrested more swiftly. The macrocracks are diverted or divided into several propagatin cracks. The increased fracture surface produced by diverting or dividing a propagating crack absorbs more energy with less structural damage [17,18].

Chapter IV

EXPERIMENTAL

To obtain a complete assessment of refractory performance, it would have been desirable to subject specimens of RFG to thermal cycling in the presence of the corrosive/erosive coal slag and seed environments present in MHD air preheaters. The experimental difficulties associated with that type of operation were prohibitive. The scope of this material study was limited to obtaining a quantitative description of the resistance of RFG to the detrimental damage caused by high temperatures and multiple thermal shock cycles.

Preheater Conditions

The anticipated operating temperatures and stress levels of the MSU experimental MHD preheater were chosen as the specific conditions to be simulated. The ceramic core of the MSU preheater was expected to operate at temperatures ranging between 1000 K and 1800 K. A web stress analysis was used to establish gas flow conditions that would limit the maximum thermally induced tensile stress level in the ceramic core [19]. Two cases were investigated, one producing a maximum tensile stress of 13.8 MPa and the other a maximum tensile stress of 34.5 MPa. Thermal cycling of the preheater would be accompanied alternately by the reducing and oxidizing atmospheres of the exhaust gases and combustion air.

Specimens (RFG)

Samples of RFG were core drilled from two different batches of as received sintered bricks. The samples were taken from a number of bricks in each batch and from a variety of locations in the bricks. While this procedure introduced another variable into the experiment, it was desired to obtain an average response of the refractory to thermal cycling. Samples with obvious flaws such as large cracks or pieces missing were rejected.

The right cylinders produced by core drilling were approximately 16.6 mm in diameter and 74.9 mm in length.

Development

A bench scale thermal stress test was developed to determine the damage resistance of RFG ceramic. The experiment was designed to operate at temperatures that would span the range found in the MSU preheaters and to produce comparable stress levels. The base temperatures chosen were 1050 K, 1400 K, and 1673 K.¹ Samples were to be cycled between temperatures near the base temperatures to generate a desired stress level. The 34.5 MPa, worst case, stress level in the

¹Available furnaces were limited to a maximum operating temperature of 1673 K.

MSU preheater was selected as the experimental stress level. The experiments were conducted in an oxidizing, air atmosphere only.

Stress Model

To achieve adequate control of the thermal stress levels generated in the experiment required a detailed heat transfer and thermo-elastic stress analysis (refer to Theory, Equations 2-10 and Appendix 3). A computer model was developed for that purpose and used to calculate the ambient temperature differences and cycle times necessary to produce the desired stress level during thermal cycling.

Initial modeling with available material properties established the operating parameters for the experiment that are given in Table 1. The ambient temperature differences and cycle times were matched to generate initial and cyclic maximum tensile stresses on the sample surface of between 33 and 36 MPa. The surface stress levels were allowed to dissipate to one-half of maximum before cycling was continued. Case 4 was added to the study after preliminary tests under the conditions of Case 3 produced extreme refractory strength degradation. The ΔT of Case 4 resulted in a drop of maximum stress level by approximately one half.

Detailed information on the material properties of RFG has recently become available, specifically on the thermal expansion coefficient and the thermal transport properties. Observation of the

TABLE 1

EXPERIMENTAL PARAMETERS

	T_B ($^{\circ}$ K)	ΔT ($^{\circ}$ K)	CT (sec)	HT (sec)
Case 1	1050	-650	85	200
Case 2	1400	-140	46	114
Case 3	1673	-100	30	90
Case 4	1673	- 50	30	90

T_B = base temperature

ΔT = ambient temperature change

CT = cyclic cooling time

HT = cyclic heating time

actual test indicated that the effect of variations in the assumed ambient temperature change needed to be included in the computer model. Nominal maximum tensile stresses were recalculated for each case, with the same ΔT and time parameters. The computer model was found to be quite sensitive to changes in the assumed material properties, particularly to variations in the thermal expansion coefficient and surface emissivity. Tensile stress levels produced by differing emissivities appear in Table 2 (see Appendix 1 for material properties). The actual emissivity of RFG is unknown, but it has been suggested that it lies between the range indicated in Table 2 and may exhibit some decrease with increasing temperature [20]. That is, surface roughness may produce an emissivity of up to .8 at lower

temperatures, but the emissivity falls off with increasing temperature as the behavior of individual phases begins to predominate.

The initial and cyclic stress levels shown in Table 2 are approximate values only. They are thermoelastic stresses calculated for a homogeneous material; which RFG is not (see Appendix 1). Calculation of these stresses assumes that the tensile strength of the material is not exceeded and fracture does not occur. Once fracture has been initiated, stress distributions are altered greatly and simplified thermoelastic solutions are no longer completely sufficient descriptions.

TABLE 2
NOMINAL MAXIMUM SURFACE STRESSES (MPa)

	$\epsilon = .5$		$\epsilon = .8$	
	Initial Stress	Cyclic Stress	Initial Stress	Cyclic Stress
Case 1	24.7	20.8	35.2	32.4
Case 2	24.9	22.2	35.7	33.6
Case 3	32.4	29.9	43.4	41.3
Case 4	16.9	15.6	22.6	21.5

ϵ = surface emissivity

Initial stress = maximum surface stress on first cooling

Cyclic stress = maximum surface stress with cyclic equilibrium

Damage Assessment

To sufficiently describe the damage resistance of RFG requires quantitative assessment of the degree of damage sustained during thermal cycling. Visual examination and three individual tests were used to measure various aspects of the damage to the ceramic microstructure.

Visual examination, both unaided and microscopic, gave a qualitative estimate of the degree and severity of cracking and changes in the refractory microstructure.

A cold compression test was used to gauge the reduction in mechanical strength of the refractory. The cold crushing strength is of little significance in high temperature applications, but it is useful for assessing the mechanical damage to the ceramic microstructure [3].

Thermal diffusivity and porosity/bulk volume measurements also gave quantitative estimates of the degree of damage to the refractory microstructure. It was hoped that these tests would provide additional correlations to the compression test and give insight to the nature of the failure mechanisms during thermal shock cycling.

Refer to Appendix 2 for descriptions of the individual tests.

Procedure

The cylindrical samples were cycled between two furnaces at different temperatures to produce the ambient temperature change associated with each case. Samples were slowly brought to temperature (+200 K/hr) and allowed to reach thermal equilibrium with the highest temperature furnace before thermal cycling was begun. The number of thermal shock cycles was varied for each sample to determine the cyclic dependence of damage sustained by the refractory. Several samples were left at 1673 K for extended periods to isolate damage due to high temperature alone. After completion of cycling, samples were slowly cooled back to room temperature (-100 to 150 K/hr). They were then examined and prepared for the damage assessment tests as described in Appendix 2.

Apparatus

The experimental apparatus for temperature cycling was similar for all four cases and is represented schematically by Figure 1.

Samples were held horizontally in the furnaces with a notched alumina tube and platinum wire pin as shown in Figure 2. Cycling between furnaces was accomplished with a push rod and a compressed air cylinder. Pressure in the cylinder was controlled by a timer and solenoid valve. A guard heater or insulator was included to reduce

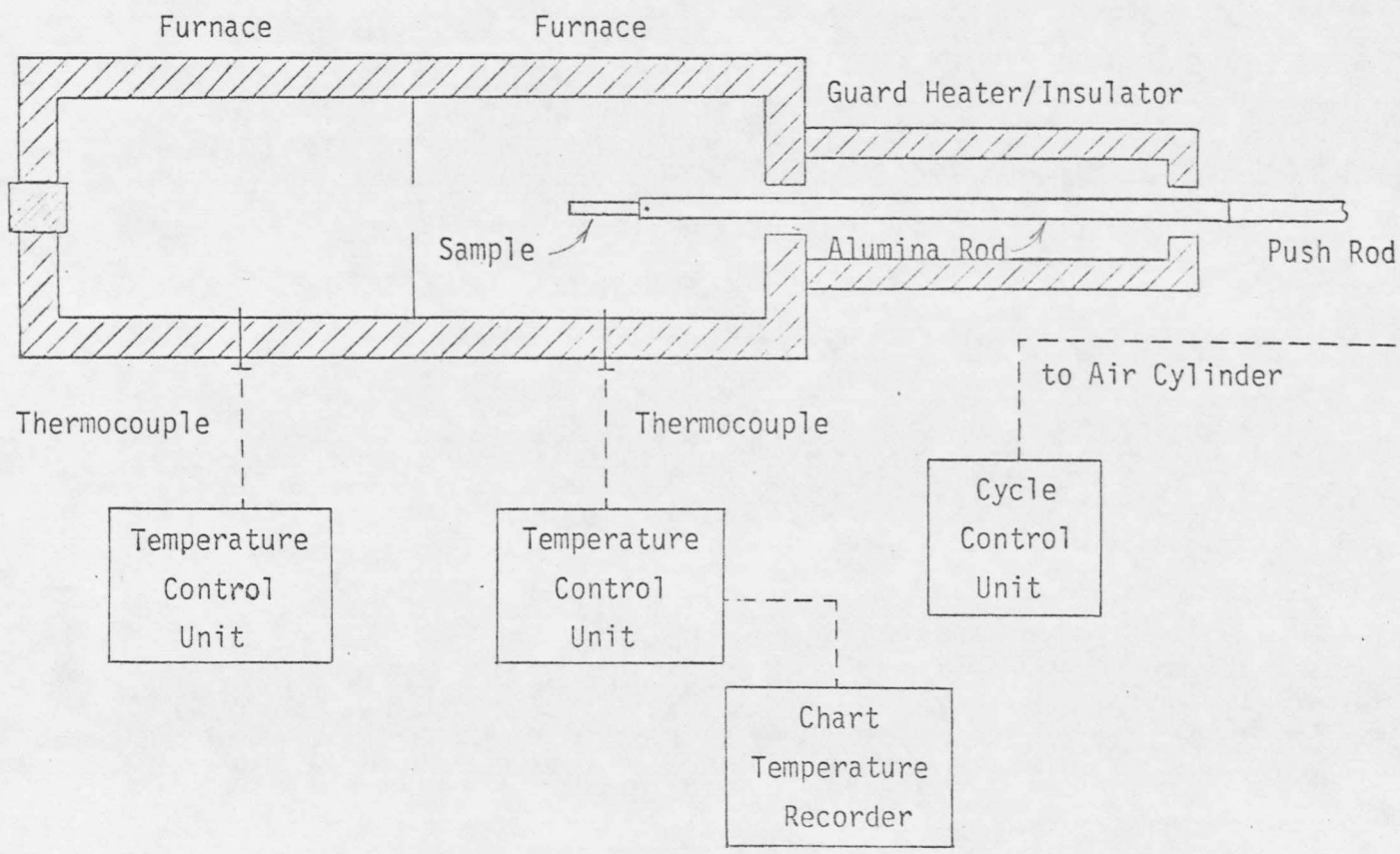


Figure 1. Experimental Apparatus

